



# Light-sensitive PEG hydrogel with antibacterial performance for pacemaker pocket infection prevention

Yurong Xiong<sup>a,b,c</sup>, Qingyun Zhang<sup>a,b,c</sup>, Juan Li<sup>a,b,c</sup>, Nan Zhang<sup>d</sup>, Xiaoshu Cheng<sup>a,b,c</sup>,  
Quanbin Dong<sup>a,\*</sup>, Huihui Bao<sup>a,b,c,\*\*</sup>

<sup>a</sup> Department of Cardiovascular Medicine, The Second Affiliated Hospital of Nanchang University, Nanchang Jiangxi, China

<sup>b</sup> Jiangxi Provincial Cardiovascular Disease Clinical Medical Research Center, Nanchang Jiangxi, China

<sup>c</sup> Jiangxi Sub-center of National Clinical Research Center for Cardiovascular Diseases, China

<sup>d</sup> Jiangxi Province Key Laboratory of Laboratory Medicine, Department of Clinical Laboratory, The Second Affiliated Hospital of Nanchang University, Nanchang, 330047, Jiangxi, China

## ARTICLE INFO

### Keywords:

2'-O-Hydroxypropyl trimethyl ammonium chloride chitosan  
Polyethylene glycol  
Cardiovascular implantable electronic device pocket infection  
Light-sensitive antibacterial hydrogel

## ABSTRACT

Prevention of cardiovascular implantable electronic devices (CIED) infection is crucial for successful outcomes. In this study, we report an adhesive and antibacterial hydrogel coating for CIED infection treatment, by immobilizing polyethylene glycol (PEG) and 2'-O-hydroxypropyl trimethyl ammonium chloride chitosan (HAC) on Ti surface. Initial alkali and APTES treatment caused the formation of  $-NH_2$  to enhance the adhesion of the hydrogel coating to Ti implants, followed by immobilizing a photo-cross-linkable PEG/2'-O-HTACCS hydrogel on Ti/OH/ $NH_2$  surface. Surface characterization of Ti/OH/ $NH_2$  sample and adhesion testing of hydrogel on Ti/OH/ $NH_2$  surface confirm successful immobilization of hydrogel onto the Ti/OH/ $NH_2$  surface. In vitro and in vivo antimicrobial results exhibited that the photo-cross-linkable PEG/HAC composite hydrogel has excellent antimicrobial capabilities against both Gram-positive (*S. aureus* and *S. epidermidis*) and Gram-negative (*P. aeruginosa* and *E. coli*) bacteria. The outcome of this study demonstrates the photo-cross linked PEG/HAC coating hydrogels can be easily formed on the Ti implants, and has great potential in preventing CIED pocket infection.

## 1. Introduction

Cardiovascular implantable electronic devices (CIED) are widely used for the treatment of arrhythmia and heart failure [1,2]. However, CIED-related infection is a major complication, which result in increased mortality and health care utilization [3]. The results from epidemiological studies showed that the incidence of CIED infection has been increasing year by year [4,5]. Pathogenic bacteria such as coagulase-negative staphylococci, staphylococcus aureus, enterococcus and pseudomonas are most common pathogens isolated in patients with CIED infection [6,7].

Currently, guidelines for prevention of CIED infection mainly recommend prophylactic systemic antibiotics [8]. However, bacteria colonized in the packet are challenging to kill with systemic antibiotics therapy, especially after the formation of bacterial biofilm. The TYRX

antibacterial envelope, which constructed from a multifilament knitted mesh with minocycline and rifampin, was approved by FDA for the prevention of CIED infection [9]. Overall, this envelop can reduce 1-year CIED infection by releasing antibiotics for 7–10 days and can be absorbed in 9 weeks. Nevertheless, a larger subcutaneous space is required when using the TYRX envelope, which increases the risk of incision dehiscence [10]. Moreover, the long-term stimulation of the surrounding tissues by the multifilament knitted mesh can might result in tissues fibrosis. Another study devised a plasma-based material (PBM) combined with antibiotics used in the prevention of CIED infection [11]. Compared to antibacterial envelop, the PBM is softer and more easily absorbed. However, long-term acquisition and preservation of plasma-based material is difficult. Moreover, antimicrobial resistance is a serious global problem and its development is driven through overuse of antibiotics. Recently, our team designed an injectable hydrogel that

\* Corresponding author. Department of Cardiovascular Medicine, the Second Affiliated Hospital of Nanchang University, No. 1 Minde Road, Nanchang Jiangxi, 330006, China.

\*\* Corresponding author. Department of Cardiovascular Medicine, the Second Affiliated Hospital of Nanchang University, Nanchang of Jiangxi, China. No. 1 Minde Road, Nanchang Jiangxi, 330006, China.

E-mail addresses: [dongquanbin@163.com](mailto:dongquanbin@163.com) (Q. Dong), [huihui\\_bao77@126.com](mailto:huihui_bao77@126.com) (H. Bao).

<https://doi.org/10.1016/j.mtbio.2024.100987>

Received 11 October 2023; Received in revised form 18 January 2024; Accepted 29 January 2024

Available online 7 March 2024

2590-0064/© 2024 Published by Elsevier Ltd. This is an open access article under the CC BY-NC-ND license (<http://creativecommons.org/licenses/by-nc-nd/4.0/>).

significantly reduces the risk of CIED infection [12]. However, the injectable hydrogels often exhibit poor encapsulation and uneven distribution in packet. Therefore, it is important to develop an antibacterial material with safe, adhesiveness and long-term stability for CIED infection.

The construction of antimicrobial coatings on the surface of implant is considered to be an effective method to inhibit bacterial attachment and biofilm formation [13,14]. Numerous materials have been studied for building antimicrobial coatings, such as polysaccharide polymers, antimicrobial peptides, and metal nanoparticles [15–17]. Chitosan is a non-toxic biological material obtained through deacetylation of chitin, and it has wide spectrum antimicrobial activity due to its polycationic nature [18–20]. However, chitosan is insoluble in water, which limits its various biomedical applications [21]. 2'-O-hydroxypropyl trimethyl ammonium chloride chitosan (HAC) is a chitosan derivative, which enhances antibacterial activity and solubility [22,23]. However, HAC hydrogel have short-term adhesiveness and poor mechanical properties.

Polydopamine (PDA) is widely used in the biomedical and pharmaceutical fields as an intermediate coating to enhance adhesion to materials [24–26]. However, PDA coating has the following shortcomings: low formation rate of coatings and uneven distribution on the material surface [27]. Hydrogel are hydrophilic polymer biomaterial, which play a significant role in the drug-delivery technology [28]. Polyethylen glycol (PEG) has been extensively applied in the preparation of hydrogels due to its biocompatibility and low immunogenicity [29]. Moreover, PEG has been widely used for reducing bacteria adhesion because of the steric barrier and excluded volume effects [30]. Numerous past studies have demonstrated that PEG is able to significantly decrease the adhesion of bacteria, such as *Staphylococcus aureus*, *Staphylococcus epidermidis*, *Escherichia coli* and *Pseudomonas aeruginosa* [31,32].

For clinical applications, it is important to complete surface modification of CIED quickly before the surgery. The photo-crosslinkable hydrogel is viewed as a promising biomaterial because of its advantages of rapid polymerization and easy controlled polymerization [33]. In this study, PEG was selected as the backbone macromolecule and then *o*-nitrobenzyl alcohol (NB) was modified to synthesize PEG-NB as previously described [34]. In addition, the hydrogel should have strong adhesion to CIED surfaces, especially in subcutaneous packet. The CIED

shell consists mainly of titanium alloy, alkali-based treatment and APTES-silanized treatment was used to generate amino ( $-\text{NH}_2$ ) on Ti surface, which build a bridge between the functional species like imine photo-crosslinkable PEG, HAC and Ti surface (Scheme 1). Under UV irradiation, the *o*-nitrobenzene in PEG-NB is converted to *o*-nitrosobenzaldehyde groups, which can subsequently react with amino groups of Ti samples and HAC. An extensive characterization of the PEG-NB/HAC composite hydrogel, including mechanical properties, in vitro and in vivo antibacterial activities, was performed. Our results show that the PEG-NB/HAC hydrogel possess promising potential for protection of CIED infection due to its excellent antibacterial capabilities and biocompatibility.

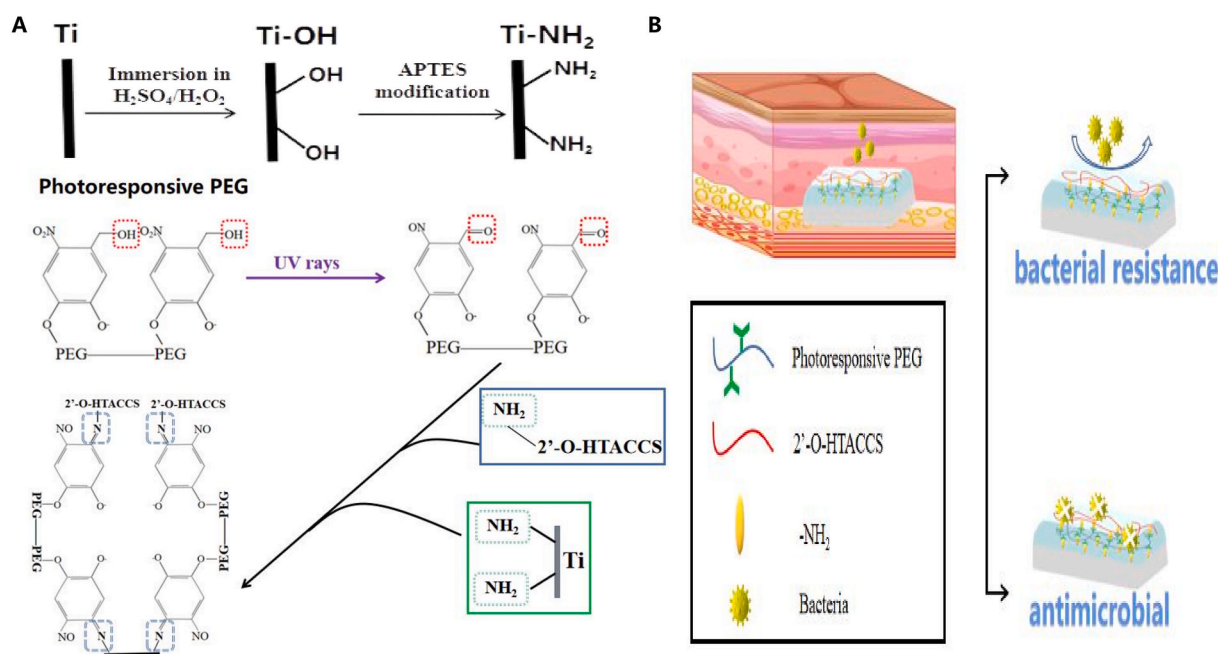
## 2. Materials and methods

### 2.1. Materials

$\beta$ -chitin, 3-chloro-2-hydroxypropyl trimethyl ammonium chloride (CTA), 3-aminopropyltriethoxysilane (APTES), HCl, isopropyl alcohol, acetone, potassium dichromate, and silver nitrate were purchased from MACKLIN reagent (Shanghai, China). All the bacteria were obtained from American Type Culture Collection (ATCC, USA). NIH-3T3 mouse fibroblast cells were kindly provided by Stem Cell Bank, Chinese Academy of Science. Live/Dead Viability/Cytotoxicity Kit (L3224), Live/Dead BacLight Bacterial Viability Kits (L7012), phosphate buffer saline (PBS), dulbecco's modified Eagle's medium (DMEM), fetal bovine serum (FBS), nutrient agar and tryptic soy broth (TSB) were purchased from Thermo Fisher Scientific (USA). Other reagents were used as received without further purification.

### 2.2. APTES attachment to titanium

The CIED including permanent cardiac pacemakers (PM), implantable cardioverter defibrillators (ICD), cardiac resynchronization therapy (CRTP), cardiac resynchronization therapy defibrillators (CRTD), and all the CIED shell is primarily composed of titanium alloy. Therefore, we used Ti sample as an alternative to CIED in this study.  $1.5 \times 1.5 \text{ cm}^2$  titanium (Ti) plates were cleaned in ethanol followed by ultrapure



**Scheme 1.** Synthesis and application of PEG-NB/HAC hydrogel. (A) Schematic of Ti/NH<sub>2</sub> samples formation and photocrosslinking of PEG-NB/2'-O-HTACCS hydrogel prepolymer solution with Ti/NH<sub>2</sub> samples. (B) Schematic representation of PEG-NB/HAC hydrogel for pacemaker pocket infection prevention.

water. Then, the Ti plates were hydroxylated in a solution of 1:1 (v/v) concentrated sulfuric acid ( $H_2SO_4$ ) and hydrogen peroxide ( $H_2O_2$ ) for 2 min [35]. They were then rinsed with DI water, and weathered. Afterward, the hydroxylated samples were further placed in APTES solution (5% v/v in ethanol) in a vacuum oven for 2 h [36]. The samples were then cleaned by rinsing with ethanol and DI water. The above modified substrates were named as Ti/ $NH_2$ .

### 2.2.1. Surface characterization

The surface morphology of Ti, Ti/OH and Ti/OH/ $NH_2$  were investigated through scanning electron microscopy (SEM, Japan, SU8100). Before the observation, all samples required gold-coating by sputtering. The surface elemental composition was evaluated using X-ray photoelectron spectroscopy (XPS, Thermo). The contact angle of surface of Ti, Ti/OH and Ti/OH/ $NH_2$  was measured using dynamic contact angle system (KRUSS DAS100, German). In addition, we selected SEM to explore the microstructure of PEG-NB/HAC hydrogels coating to Ti implants.

### 2.3. Synthesis of PEG-NB/HAC composite hydrogel

HAC with a high degree of functionalization was synthesized in accordance with previously reported methods [23]. The synthesis method of PEG-NB was reported according to previous literature [34, 37]. Fig. S1 demonstrates the  $^1H$  NMR spectrum of the PEG-NB. The  $^1H$  NMR spectrum of PEG-NB showed obvious peaks that corresponded to the peaks of hydrogen atoms (a, b, h, i) in NB. This result confirmed successful graft of NB to PEG. Fig. S2 presents the chemical formula of PEG-NB and HAC. Purified HAC (0.7g) and PEG-NB (1g) was successively added to 10 ml of PBS and fully dissolved overnight at 4 °C, to obtain hydrogel precursor solution (7 wt% HAC/10 wt% PEG-NB). A certain amount of hydrogel precursor solution is added to the surface of the Ti plates, upon UV exposure, o-nitrobenzene converted to o-nitrosobenzaldehyde groups, which then crosslink with amino groups of Ti samples and HAC to form cured hydrogel.

### 2.4. Adhesive test

The adhesive properties of hydrogels were measured by a visual and quantitative method. Briefly, 100  $\mu$ l PEG-NB/HAC composite hydrogels added to the surface of Ti, Ti/OH and Ti/OH/ $NH_2$ . Then, a glass sheet was placed in contact with the hydrogels to form an overlapping area of approximately  $1.5 \times 1.5$  cm<sup>2</sup>. After UV light irradiation for 30s, the lap shear test was performed by the electronic universal testing machine (CMT2102, MTS) at a tensile speed of 3 mm/min.

### 2.5. In vitro biocompatibility

The biocompatibility of PEG-NB/HAC hydrogel was assayed by a Cell Counting Kit-8 for NIH 3T3 mouse fibroblast cells. NIH 3T3 cells were cultured in 96-well culture plates at a concentration of  $\sim 1 \times 10^4$  cells per well with DMEM supplemented with 10% FBS and incubated at 37 °C in 5% CO<sub>2</sub> overnight. Then, the growth media was removed and the growth media extracts of the uncoated and hydrogel coated Ti plates which was soaked for 24h were added on the cell layer. The growth media was removed at 24h and 72h, respectively. 100  $\mu$ l of DMEM contained 10  $\mu$ l CCK-8 solution was added to each well. After 2 h of incubation, the absorbance was measured at OD<sub>450</sub>.

The biocompatibility of PEG-NB/HAC hydrogel was also evaluated by a live/dead assay kit. Briefly, 3T3 cells were cultured in 24-well overnight at a density of  $5 \times 10^4$  cells per well and then cultured in growth media extracts of the hydrogels for 24h and 72h, respectively. Each sample were stained with calcein AM (0.5  $\mu$ l/mL) and ethidium homodimer-1 (EthD-1, 2  $\mu$ l/mL) in PBS for live and dead cells, respectively. The cells were incubated at 37 °C for 20 min, followed by observed by inverted fluorescence microscope.

In addition, we added hemolytic activity assay for hydrogel to further evaluate the safety of hydrogels. Whole Blood was collected from a healthy human volunteer with written informed consent. Erythrocytes were collected by centrifugation at 1500 rpm for 15 min, washed three times with PBS, and suspended in PBS. Afterward, 1 mL of RBC suspension and 20  $\mu$ l of hydrogel were added in a tube and incubated at 37 °C for 1 h. Triton X-100 and PBS were used as positive and negative controls, respectively. The absorbance of supernatant, after centrifugation, was analyzed at 540 nm [38].

### 2.6. In vivo toxicity

All animal experiments were conducted in accordance with the guidelines of the Animal Care and Ethics Committee of Nanchang University. Sprague-Dawley (SD) rats (female, 250–350 g) were randomly divided into control groups (3 rats in each of the 1-, 7-, and 14-day groups) and experimental groups (3 rats each of the 1-, 7-, and 14-day groups). The rats in the control group were implanted with bare Ti plates and rats in the experimental group were implanted with Ti- $NH_2$  coated with hydrogels. All samples were implanted into the subcutaneous pocket on the right dorsum of the rats. At each experimental time point (1, 7, and 14 days), the tissues around the site of implantation, heart, liver, kidney, and blood samples were collected. The tissue samples were stained via H&E staining to evaluate the inflammatory response around the site of implantation. The blood samples from rats were collected for routine blood, liver and kidney function assessment. In addition, we regularly observed the in vivo degradation of the hydrogel until the hydrogel was completely dissolved.

### 2.7. In vitro antibacterial tests

Antimicrobial performance of PEG-NB/HAC hydrogel was conducted by colony counting, live/dead fluorescence staining and SEM observation with Gram-positive (*S. aureus* and *S. epidermidis*) and Gram-negative (*P. aeruginosa* and *E. coli*) bacteria. Briefly, 100  $\mu$ l of bacterial suspension ( $10^8$  cfu/ml) was introduced to three bare Ti plates and three Ti- $NH_2$  load with hydrogels, respectively. After 4 h, 24 h and 48 h of incubation, the bacterial culture were removed serially diluted with PBS for colony counting. The antimicrobial activity of hydrogel was also evaluated by fluorescence microscopy. After stained for 20 min, the bacteria on the surfaces were observed by inverted fluorescence microscope. In addition, the morphology of the adhered bacteria on the samples was observed by scanning electron microscopy (SEM).

### 2.8. In vivo antibacterial studies

To evaluate the antibacterial property of the PEG-NB/HAC composite hydrogel in vivo, this study was conducted on the pocket infection of the rat model. CIED are primarily implanted under the skin of the patient's chest in clinical practice. Therefore, we chose to implant the samples under the skin of the rat's back, which is similar to the skin structure at the location of CIED implantation in humans. Previous studies have also used the back of the animal as the implantation site for CIED [11,12,39]. *Staphylococcus aureus* is the most common cause of bacteraemia and early pocket infections. Therefore, we chose *Staphylococcus aureus* as the causative agent for the construction of an in vivo model of CIED pocket infection. The bare Ti plates and Ti- $NH_2$  plates coated with hydrogel were incubated in *S. aureus* suspension ( $1 \times 10^8$  CFU/mL) for 4 h. The back was shaved and the underlying skin was disinfected with alcohol under general anesthesia. Under sterile conditions, two subcutaneous pockets were created on both sides of the back, and the left pocket was implanted with bare Ti plates. After 3 and 7 days implant period, the samples were removed and immersed in 5 mL PBS and sonicated for 5 min. After ultrasonication, solution were diluted and plated onto agar plates for colony counting. Moreover, microbial activity on the Ti plates surface of the control and experimental group

was evaluated using fluorescence microscopy.

In addition, the tissues around the site of implantation were removed and conducted the H&E stained as described above. The expression of interleukin 1 $\beta$  (IL-1 $\beta$ ) and tumor necrosis factor  $\alpha$  (TNF- $\alpha$ ) of the pocket was tested by immunohistochemical staining. Images of stained slides were acquired using the ScanScope CT automated slide scanning system (Aperio Technologies, Vista, CA, USA). Gene expression was also assessed by Quantitative Real-Time PCR (qRT-PCR). Total RNA was purified from freshly tissue around the site of implantation via RNAprep Pure Kit (TIANGEN) and complementary DNA was synthesized using FastKing gDNA Dispelling RT SuperMix (TIANGEN). The primers used in the study were showed in Table S1. Gene expression levels were quantified by the 2- $\Delta\Delta$ CT method (Ct of target gene, Ct of GAPDH).

## 2.9. Statistical analysis

All data are shown as mean  $\pm$  standard deviation (SD). Experimental data were analyzed using one-way analysis of variance (ANOVA) with Tukey's post hoc analysis. Statistical significance was accepted for  $P$  values of  $<0.05$ .

## 3. Results and discussion

### 3.1. Surface characterizations

To determine the surface properties of samples at each stage of surface modification, we assessed the sample surfaces based on Surface topography (SEM), surface hydrophilicity (contact angle measurements) and elemental composition (XPS). Fig. 1A displays the representative

SEM images of the various treated surface morphologies. As shown in Fig. 1A, the surface of pure Ti plate was typically flat. After alkali treatment, large surface irregularities with a roughness formed on Ti surface. Compared with the hydroxyl-modified Ti, nodular structures were emerged on the surface of APTES-modified Ti. Similar structure was found in another study [36,40,41].

XPS analysis was conducted to assess the elemental composition of the different sample surfaces. Table 1 and Fig. S3 presents the results of surface elemental analysis. XPS after alkali treatment showed a significantly increase in the oxygen (O%). Modification with APTES increased nitrogen (N%), carbon (C%) and silicon (Si%) to 9.32%, 9.21% and 42.82% respectively. Moreover, APTES decreased O% to 37.19% and Ti % to 1.46%. Changes in surfaces composition indicate the successful immobilization of hydroxyl group and APTES onto the surface.

Water contact angle was assessed to identify the hydrophilicity change of various sample surfaces (Fig. 1B). The results showed that the water contact angle decreased after alkali treatment [40], as shown by a decrease in the water contact angle from  $65.5 \pm 0.51^\circ$  to  $41.3 \pm 1.0^\circ$ . The change in water contact angle was attributed to the presence of

**Table 1**

Elemental compositions (at.%) of different sample surfaces determined by XPS.

	Black	NaOH	APTES
C (%)	12.79	11.08	42.74
N (%)	0.00	0.00	9.40
O (%)	16.14	68.24	37.24
Ti (%)	71.07	20.68	1.49
Si (%)	0.00	0.00	9.14

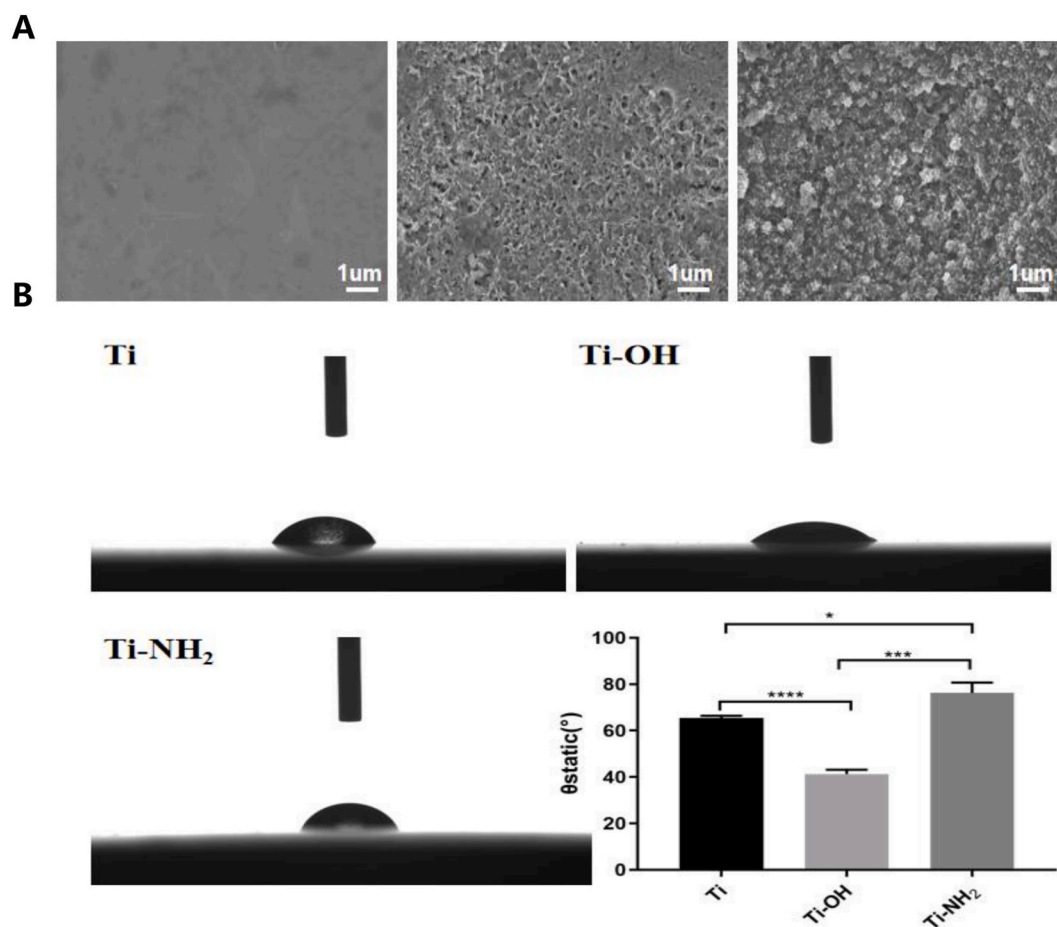


**Fig. 1.** (A) SEM images and (B) Water contact angle of Ti, Ti-OH, Ti-NH<sub>2</sub> samples. (A) The representative SEM images of the various treated surface morphologies. (B) Digital photos of the water droplets placed on surface of Ti, Ti-OH, Ti-NH<sub>2</sub> samples; Average static contact angle determined after 10 min.

numerous of hydrophilic hydroxyl groups on the alkali-treated surface [42]. The water contact angle increased to  $76.3 \pm 2.6^\circ$  after APTES modification due to APTES is hydrophobic molecular. The results also show the successful modification of hydroxyl group and APTES onto the sample surfaces.

To verify the conversion of *o*-nitrobenzene in PEG-NB to *o*-nitrobenzaldehyde groups after irradiation, it can then react with the amino groups of Ti samples and HAC. We selected SEM to explore the microstructure of PEG-NB/HAC hydrogels coating to Ti implants. Cross sections of PEG-NB/HAC hydrogels coating to Ti implants are shown in Fig. S4. It can be found that hydrogels show a highly interconnected and porous three-dimensional network structure coating to Ti implants.

### 3.2. Adhesion of PEG-NB/HAC hydrogels

High adhesion of hydrogels to Ti surfaces is important for the success of the PEG-NB/HAC hydrogel coating on Ti implants. The adhesive test was assessed by placing the hydrogels between Ti sample and glass slide according to the lap shear strength test. As shown in Fig. 2, the adhesion property of hydrogels to Ti was significantly increased after APTES modification compared to the Ti and alkali treatment groups. Results showed that lap shear strengths was enhanced after APTES modification from  $13.2 \pm 0.6$  kPa to  $38.7 \pm 1.3$  kPa. The almost 2-fold increase in adhesion property after APTES modification might be attributed to the binding effect between the amino groups and hydroxyl groups, which significantly improved coating stability on Ti implants [43].

### 3.3. Biocompatibility assay

The hydrogel kills bacteria through a direct contact mechanism, which maybe damage mammalian cells. The live/dead cell staining and CCK-8 assay were performed to assess the cytotoxicity of PEG-NB/HAC hydrogels. Fig. 3A shows the live/dead fluorescent images of 3T3 cells. The overall cell viability was similar between control and hydrogel groups at days 1 and 3 of culture. Furthermore, high cell viability (>90%) was observed in all groups after culturing for 1, 3 and 7 days (Fig. 3B), indicating that the hydrogel shows excellent biosafety [44]. As shown in Fig. S5, the PEG-NB/HAC hydrogels produced negligible hemolysis, indicating that PEG-NB/HAC hydrogels exhibited good hemocompatibility.

The degradation products of the hydrogel can be absorbed into the circulatory system, so it is important to assess the biocompatibility of hydrogel. The histocompatibility of the hydrogel was evaluated in rats. Ti plates and Ti-NH<sub>2</sub> coated with hydrogels were implanted in the back of the rats under a sterile environment. H&E staining of the tissues around the site of implantation, heart, liver and kidney were evaluated

after 1d, 7d, and 14 d. As shown in Fig. 3C and Figs. S6–S9, there were no obvious toxicity and inflammatory reaction in experimental group compared with the control group. The biosafety was also assessed by blood routine, liver function and renal function. There were no significant difference in white blood cell (WBC), red blood cell (RBC), alanine aminotransferase (ALT) and serum creatinine between control group and experimental group (Fig. 3D). Furthermore, other biomarkers of blood routine (platelet and hemoglobin), hepatic (aspartate aminotransferase, glutamyl transpeptidase and bilirubin) and renal function (blood urea nitrogen) were normal in hydrogel group (Fig. S10). The in situ hydrogel was surgically separated and observed. As shown in Fig. S11, the PEG-NB/HAC hydrogel adhering to Ti sheets could be completely degraded in vivo within 10 days. According to the above results, PEG-NB/HAC hydrogel has high biological safety.

### 3.4. In vitro antibacterial activity

Previous studies have suggested an increased rate of CIED-related infection and antibiotic resistance [5,45]. In present study, instead of using antibiotics, we used PEG-NB/HAC composite hydrogel to achieve the purpose of preventing CIED infection. The antimicrobial activity of the PEG-NB/HAC hydrogel was first evaluated via colony count. Representative bacteria of CIED-associated infections, Gram-positive (*S. aureus* and *S. epidermidis*) and Gram-negative (*P. aeruginosa* and *E. coli*) bacteria were used to evaluate the antimicrobial capability of the PEG-NB/HAC composite hydrogels using the colony counting assay [46]. After 4, 24 and 48h of incubation, the colonies were counted and compared with the control group. As shown in Fig. 4A and Fig. S12A, the results of colony count are presented as images and histograms. For all four species of bacteria used in the experiment, the control groups displayed significant increased colony counts during incubation, as expected. In contrast, PEG-NB/HAC composite hydrogel exhibited excellent antimicrobial capability, the colony counts of hydrogel groups was significantly lower than control groups.

The antibacterial activity of the PEG-NB/HAC hydrogel was further assessed by a live/dead bacterial staining. Four different bacteria were incubated on the surface of hydrogel coatings for 24 h, and Ti samples were used as the control groups. Living bacteria were stained as green and dead as red, respectively. As shown in Fig. 4B and Fig. S12B, bacteria incubated on the surface of Ti plates were shown very high viability after 24 h. In contrast, the results from the PEG-NB/HAC composite hydrogel were found to have a lower viability for four different bacteria.

The antibacterial properties of chitosan are mainly attributed to polycationic nature, which disrupts the integrity of the outer membrane and ultimately leads to cell death [18]. Moreover, PEG possess the ability to resist bacterial adhesion and inhibit biofilm formation [32]. To

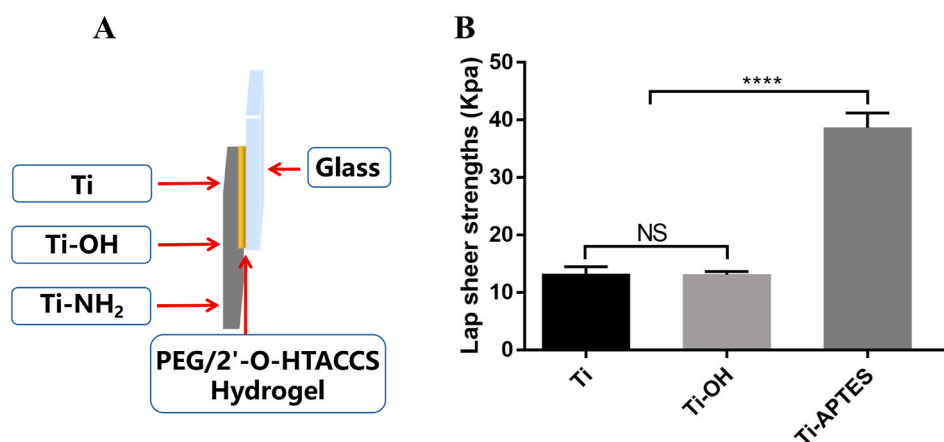
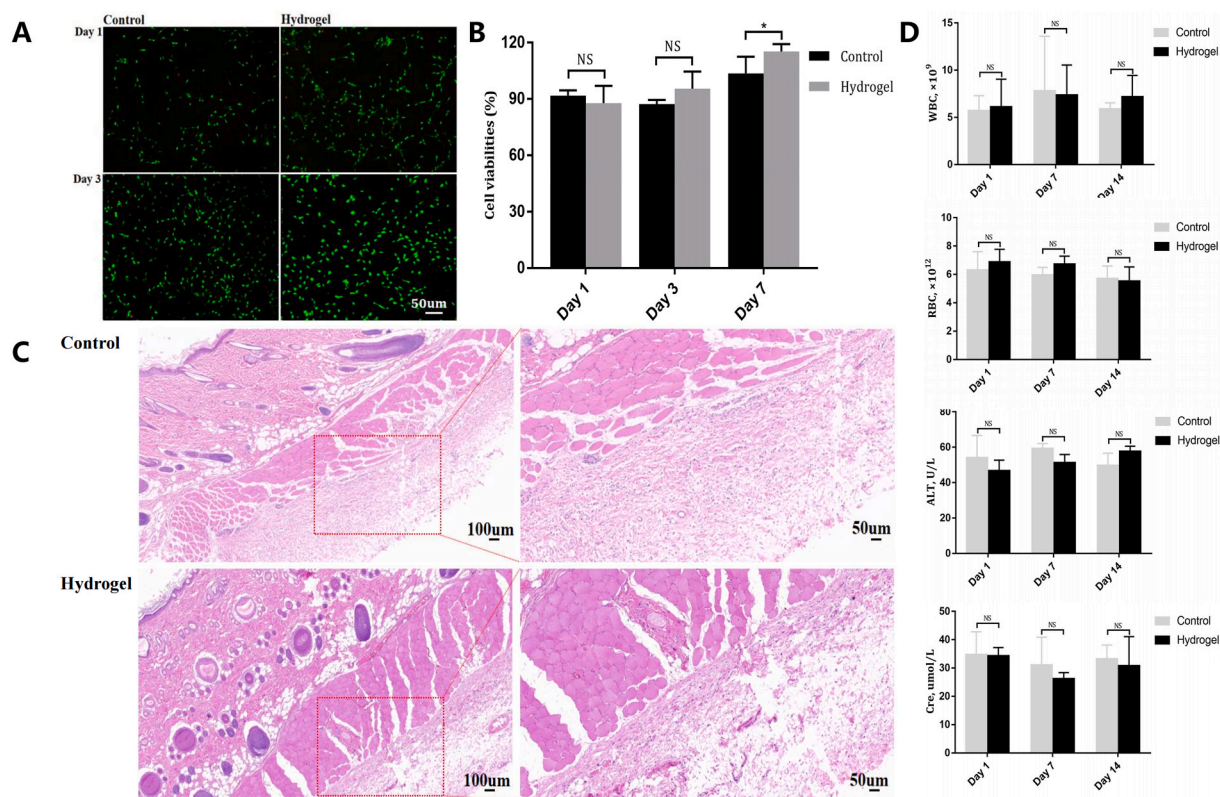
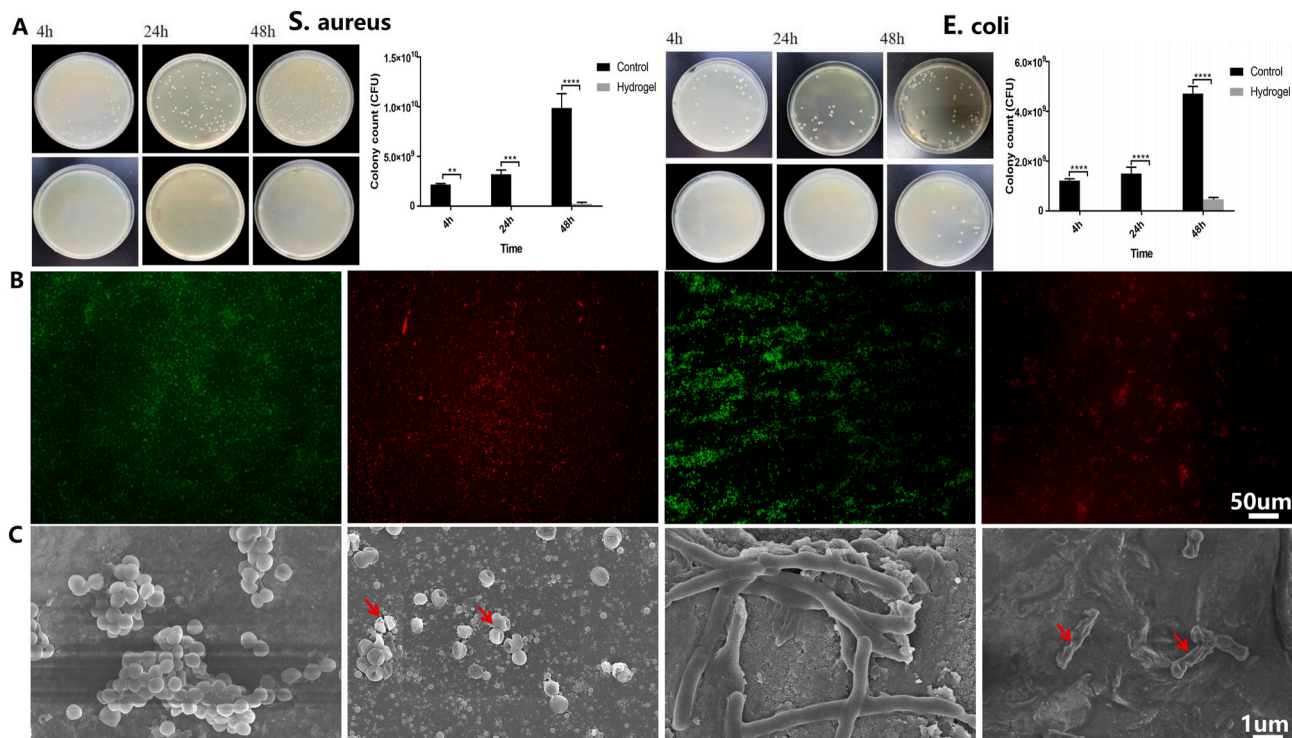


Fig. 2. Adhesion properties of PEG-NB/HAC hydrogel to different Ti samples. (A) Schematic presentation of the lap shear test; (B) Lap shear strengths of PEG-NB/HAC hydrogel of to different Ti samples.



**Fig. 3.** Biocompatibility of PEG-NB/HAC hydrogel. (A) Live/Dead staining images and (B) Cell viability of fibroblast cells after coculture with hydrogels. (C) H&E staining of tissue around the site of implantation. (D) White blood cell, red blood cell, alanine aminotransferase and serum creatinine in rats after implantation of hydrogel. (\* $P < 0.05$ )



**Fig. 4.** In vitro antibacterial activity of the PEG-NB/HAC hydrogel. (A) Bacteria colony count experiments, (B) Live/dead bacterial viability assay, and (C) SEM images of *S. aureus* and *E. coli* after co-culture with the PEG-NB/HAC hydrogel.

better understand the antibacterial mechanism of the PEG-NB/HAC composite hydrogels, SEM was used to observe the morphological change of the bacteria in contact with the hydrogels [47]. The SEM images presented for control groups showed that bacteria retained smooth spherical morphologies with intact membranes after 24 h of incubation (Fig. 4C and Fig. S12C). In contrast, only few bacteria were able to adhere to the PEG-NB/HAC composite hydrogels coating surfaces. Moreover, the bacteria on the hydrogels coating surfaces exhibited morphological deformations. Considering the high initial number of bacteria ( $10^7$  cfu/mL), the PEG-NB/HAC composite hydrogels coating might be effective in clinical situations.

### 3.5. In vivo antibacterial activity

A rat model of CIED pocket infection was developed to investigate the antimicrobial capability of PEG-NB/HAC hydrogel in vivo (Fig. 5A). The treatment was divided into control and PEG-NB/HAC hydrogel groups. After 3 and 7 days implant period, the pockets were opened for observation, and the Ti samples collected in pockets were assessed for bacterial infection using live/dead staining and colony counting. Fig. 5B shows the representative images of *S. aureus*-infected pockets after 3 and 7 days. The control group was found to have pus accumulation in the pockets. In contrast, there were no purulence in the hydrogel groups, which could be attributed to their effective antibacterial activity. AS shown in Fig. 5C, Live/dead staining revealed that the bacteria viability of the control groups was clearly visible by green fluorescence, while the bacteria membrane permeability was enhanced in the hydrogel groups, as seen by red fluorescence. The antibacterial activity of PEG-NB/HAC composite hydrogels coated on Ti plates was assessed by colony counting assay. On days 3 and 7, the bacterial burden collection from the Ti samples was compared between control groups and hydrogel groups. A large number of colonies were found on the agar plates in the control groups, whereas few colonies were found in the hydrogel groups (Fig. 5D). These results suggested that PEG-NB/HAC hydrogels had excellent antibacterial activities for CIED related infection.

On the days 3 and 7, the tissues around the pocket were collected and stained with H&E, IL-1 $\beta$ , and TNF- $\alpha$ , and further studied for inflammatory gene expression by qRT-PCR [48,49]. H&E staining of the tissues in the site of implantation showed that there was substantial inflammatory cell infiltration and purulent phenomenon in control groups. In the PEG-NB/HAC composite hydrogels groups, there were no significant exudation and inflammatory reactions in the fascia (Fig. 6A and Fig. S13). In addition, in the case of IL-1 $\beta$  and TNF- $\alpha$  staining, a significant reduction of inflammatory cytokines (brown staining) was observed in the hydrogel groups, while severe inflammation response was observed in control group (Fig. 6B). Quantitative RT-PCR (qPCR) revealed that the mRNA levels of IL-1 $\beta$  and TNF- $\alpha$ , two inflammatory factors, markedly higher in the control groups than in the hydrogel groups (Fig. 6C). In summary, inflammatory responses of the tissues around the pocket were significantly lower in hydrogel groups [50]. These in vivo results indicated the PEG-NB/HAC composite hydrogel can inhibit bacterial growth and accumulation on the Ti implants, which is promising for avoiding CIED related infection.

## 4. Conclusion

In this study, we designed a photo-cross linked PEG-NB/HAC coating hydrogel for Ti implants to prevent CIED related infection. Alkali-based and APTES treatment caused the formation of -NH<sub>2</sub> to enhance the adhesion of the hydrogel coating to Ti implants. After coating onto the Ti surface, the hydrogel coating is easily crosslinking between *o*-nitrosobenzaldehyde groups of PEG-NB and amino groups of HAC and Ti samples upon UV irradiation. These in vitro and in vivo results suggested that the biocompatibility and antibacterial activity of the PEG-NB/HAC hydrogels. When applied in a CIED pocket infection model, the photo-cross linked hydrogel was found to significantly inhibit implant-related infections. In summary, our study shows that the photo-cross linked PEG-NB/HAC coating hydrogel can be easily formed on the Ti implants, and has great potential in preventing CIED pocket infection.

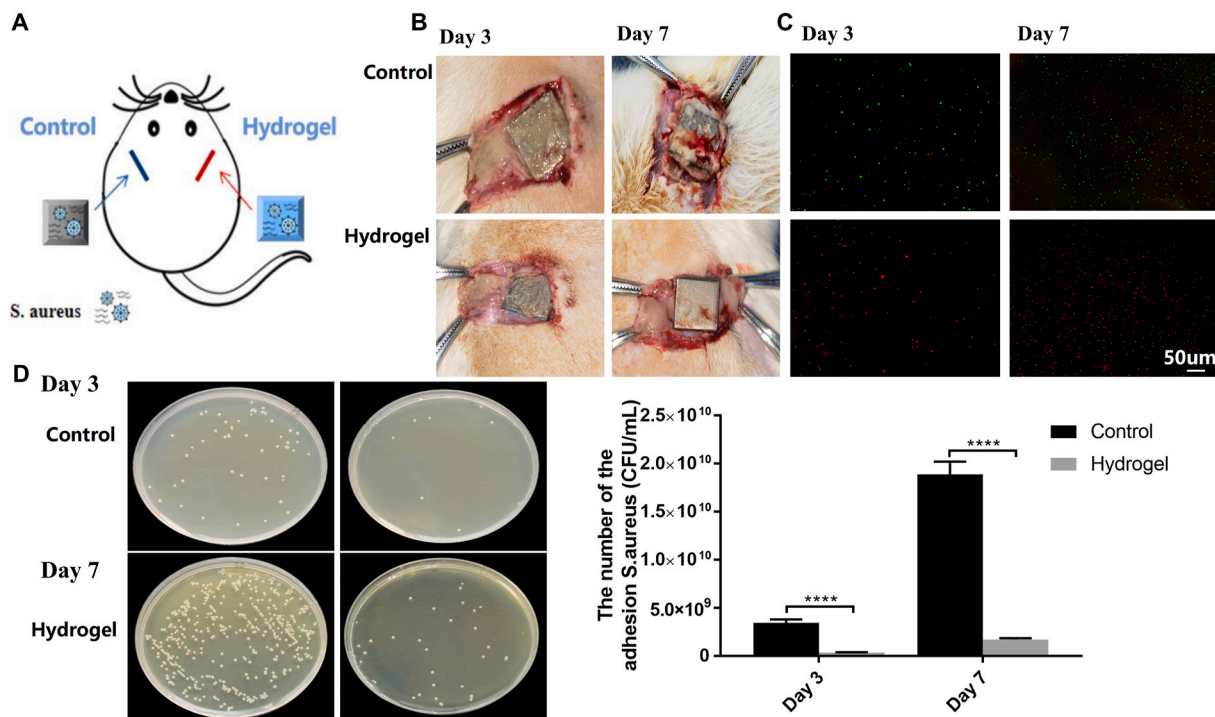
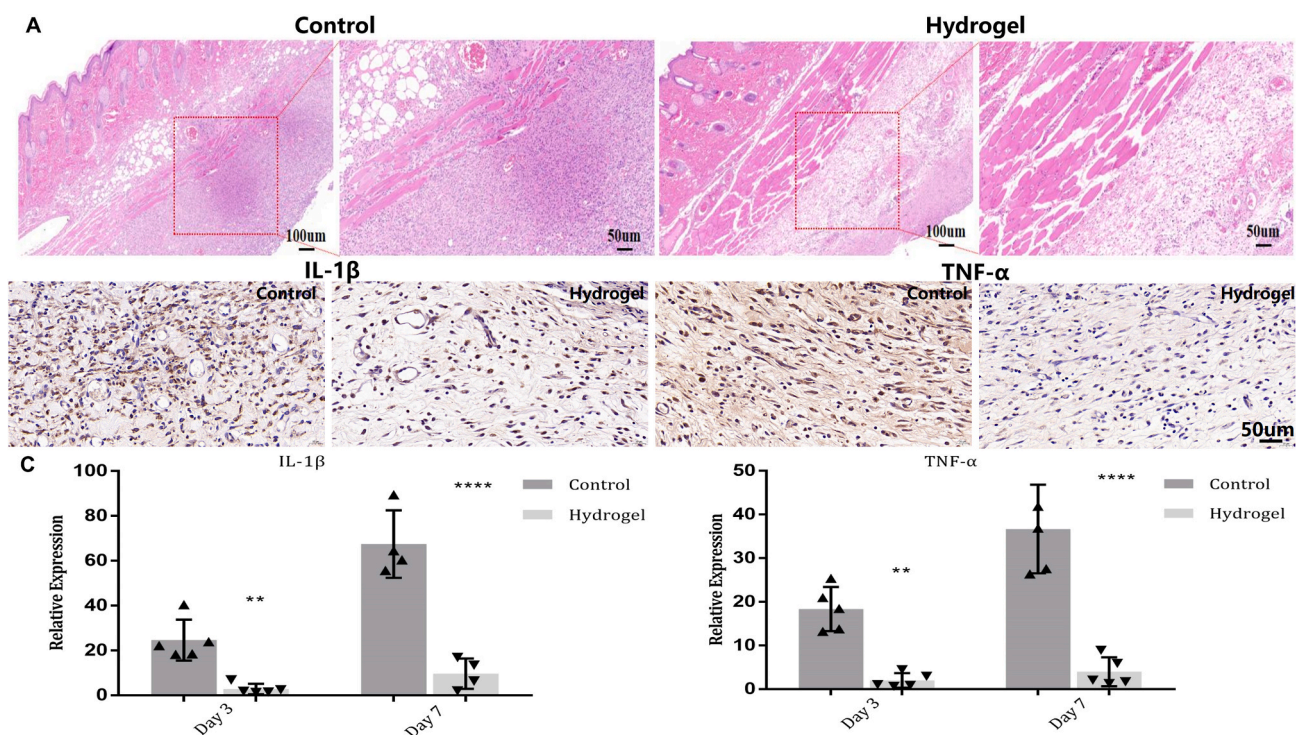


Fig. 5. In vivo antibacterial activity of the PEG/HAC hydrogel. (A) Schematic illustration of PEG-NB/HAC hydrogel for prevention of pocket infection. (B) The image of the pockets in visually. (Day 3 and Day 7) (C) Live/dead bacterial viability assay of the Ti implants. (D) The plate for bacterial count of the control group and PEG-NB/HAC hydrogel group at different time.



**Fig. 6.** Histological, immunohistochemical and qRT-PCR evaluation of tissue around the site of implantation in different groups. (A) Representative images of tissues around the pocket with H&E, IL-1 $\beta$ , and TNF- $\alpha$  staining on day 7. (B) Real-time PCR analysis of inflammation cytokines level (IL-1 $\beta$  and TNF- $\alpha$ ) of tissues around the pocket.

#### CRediT authorship contribution statement

**Yurong Xiong:** Investigation, Resources, Validation, Writing – original draft. **Qingyun Zhang:** Investigation, Validation. **Juan Li:** Methodology. **Nan Zhang:** Methodology. **Xiaoshu Cheng:** Conceptualization, Methodology, Resources. **Quanbin Dong:** Conceptualization, Methodology, Resources. **Huihui Bao:** Conceptualization, Funding acquisition, Investigation, Methodology, Project administration, Writing – review & editing.

#### Declaration of competing interest

The authors declare that they have no known competing financial interests or personal relationships that could have appeared to influence the work reported in this paper.

#### Data availability

Data will be made available on request.

#### Acknowledgments

This work was supported by National Natural Science Foundation of China (82160070), Natural Science Foundation of Jiangxi Province of China (20192BAB205033, 20224BAB206090, S2021ZRZDL0178). The authors thank professor Linyong Zhu and his team for the guidance on chemical synthesis.

#### Appendix A. Supplementary data

Supplementary data to this article can be found online at <https://doi.org/10.1016/j.mtbio.2024.100987>.

#### References

- [1] C. Linde, W.T. Abraham, M.R. Gold, M. St John Sutton, S. Ghio, C. Daubert, R. S. Group, Randomized trial of cardiac resynchronization in mildly symptomatic heart failure patients and in asymptomatic patients with left ventricular dysfunction and previous heart failure symptoms, *J. Am. Coll. Cardiol.* 52 (2008) 1834–1843.
- [2] S. Cazeau, C. Leclercq, T. Lavergne, S. Walker, C. Varma, C. Linde, S. Garrigue, L. Kappenberger, G.A. Haywood, M. Santini, C. Bailleul, J.C. Daubert, I. Multisite Stimulation in Cardiomyopathies Study, Effects of multisite biventricular pacing in patients with heart failure and intraventricular conduction delay, *N. Engl. J. Med.* 344 (2001) 873–880.
- [3] C.H. Cabell, P.A. Heidenreich, V.H. Chu, C.M. Moore, M.E. Stryjewski, G.R. Corey, V.G. Fowler Jr., Increasing rates of cardiac device infections among Medicare beneficiaries: 1990–1999, *Am. Heart J.* 147 (2004) 582–586.
- [4] J.B. Johansen, O.D. Jørgensen, M. Møller, P. Arnsbo, P.T. Mortensen, J.C. Nielsen, Infection after pacemaker implantation: infection rates and risk factors associated with infection in a population-based cohort study of 46299 consecutive patients, *Eur. Heart J.* 32 (2011) 991–998.
- [5] A.J. Greenspon, J.D. Patel, E. Lau, J.A. Ochoa, D.R. Frisch, R.T. Ho, B.B. Pavri, S. M. Kurtz, 16-Year Trends in the infection burden for pacemakers and implantable cardioverter-defibrillators in the United States: 1993 to 2008, *J. Am. Coll. Cardiol.* 58 (2011) 1001–1006.
- [6] R. Margey, H. McCann, G. Blake, E. Keelan, J. Galvin, M. Lynch, N. Mahon, D. Sugrue, J. O'Neill, Contemporary management of and outcomes from cardiac device related infections, *Europace* 12 (2010) 64–70.
- [7] M.G. Bongiorno, C. Tascini, E. Tagliaferri, A. Di Cori, E. Soldati, A. Leonildi, G. Zucchelli, I. Ciullo, F. Menichetti, Microbiology of cardiac implantable electronic device infections, *Europace* 14 (2012) 1334–1339.
- [8] C. Blomström-Lundqvist, V. Traykov, P.A. Erba, H. Burri, J.C. Nielsen, M. G. Bongiorno, J. Poole, G. Boriani, R. Costa, J.-C. Deharo, L.M. Epstein, L. Saghly, U. Snygg-Martin, C. Starck, C. Tascini, N. Strathmore, European heart rhythm association (EHRA) international consensus document on how to prevent, diagnose, and treat cardiac implantable electronic device infections—endorsed by the heart rhythm society (HRS), the asia pacific heart rhythm society (APHRS), the Latin American heart rhythm society (LAHRS), international society for cardiovascular infectious diseases (ISCVID), and the European society of clinical microbiology and infectious diseases (ESCMID) in collaboration with the European association for cardio-thoracic surgery (EACTS), *Eur. Heart J.* 41 (2020) 2012–2032.
- [9] K.G. Tarakji, S. Mittal, C. Kennergren, R. Corey, J.E. Poole, E. Schloss, J. Gallastegui, R.A. Pickett, R. Evonich, F. Philippon, J.M. McComb, S.F. Roark, D. Sorrentino, D. Sholevar, E. Cronin, B. Berman, D. Riggio, M. Biffi, H. Khan, M. T. Silver, J. Collier, Z. Eldadah, D.J. Wright, J.D. Lande, D.R. Lexcen, A. Cheng, B.

- L. Wilkoff, W.-I. Investigators, Antibacterial envelope to prevent cardiac implantable device infection, *N. Engl. J. Med.* 380 (2019) 1895–1905.
- [10] D.S. Hirsh, H.L. Bloom, Clinical use of antibacterial mesh envelopes in cardiovascular electronic device implantations, *Med Devices (Auckl)* 8 (2015) 71–78.
- [11] D. Schwartzman, A.W. Pasculle, K.D. Ceceris, J.D. Smith, L.E. Weiss, P. G. Campbell, An off-the-shelf plasma-based material to prevent pacemaker pocket infection, *Biomaterials* 60 (2015) 1–8.
- [12] Q. Dong, X. Zhong, Y. Zhang, B. Bao, L. Liu, H. Bao, C. Bao, X. Cheng, L. Zhu, C. Lin, Hyaluronic acid-based antibacterial hydrogels constructed by a hybrid crosslinking strategy for pacemaker pocket infection prevention, *Carbohydr. Polym.* 245 (2020) 116525.
- [13] Z.X. Voo, M. Khan, Q. Xu, K. Narayanan, B.W.J. Ng, R. Bte Ahmad, J.L. Hedrick, Y. Y. Yang, Antimicrobial coatings against biofilm formation: the unexpected balance between antifouling and bactericidal behavior, *Polym. Chem.* 7 (2016) 656–668.
- [14] S.B. Goodman, Z. Yao, M. Keeney, F. Yang, The future of biologic coatings for orthopaedic implants, *Biomaterials* 34 (2013) 3174–3183.
- [15] Y. Qian, F. Qi, Q. Chen, Q. Zhang, Z. Qiao, S. Zhang, T. Wei, Q. Yu, S. Yu, Z. Mao, C. Gao, Y. Ding, Y. Cheng, C. Jin, H. Xie, R. Liu, Surface modified with a host defense peptide-mimicking beta-peptide polymer kills bacteria on contact with high efficacy, *ACS Appl. Mater. Interfaces* 10 (2018) 15395–15400.
- [16] B. Bhattacharjee, S. Ghosh, D. Patra, J. Haldar, Advancements in release-active antimicrobial biomaterials: A journey from release to relief, *Wiley Interdiscip Rev Nanomed Nanobiotechnol* 14 (2022) e1745.
- [17] G.-A. Junter, P. Thébault, L. Lebrun, Polysaccharide-based antibiofilm surfaces, *Acta Biomater.* 30 (2016) 13–25.
- [18] I.Y. Kim, S.J. Seo, H.S. Moon, M.K. Yoo, I.Y. Park, B.C. Kim, C.S. Cho, Chitosan and its derivatives for tissue engineering applications, *Biotechnol. Adv.* 26 (2008) 1–21.
- [19] B.H. Neufeld, M.J. Neufeld, A. Lutzke, S.M. Schweickart, M.M. Reynolds, Metal-organic framework material inhibits biofilm formation of *Pseudomonas aeruginosa*, *Adv. Funct. Mater.* 27 (2017).
- [20] P. Xue, Q. Li, Y. Li, L. Sun, L. Zhang, Z. Xu, Y. Kang, Surface modification of poly (dimethylsiloxane) with polydopamine and hyaluronic acid to enhance hemocompatibility for potential applications in medical implants or devices, *ACS Appl. Mater. Interfaces* 9 (2017) 33632–33644.
- [21] D. Zhu, H. Cheng, J. Li, W. Zhang, Y. Shen, S. Chen, Z. Ge, S. Chen, Enhanced water-solubility and antibacterial activity of novel chitosan derivatives modified with quaternary phosphonium salt, *Mater. Sci. Eng., C* 61 (2016) 79–84.
- [22] J. Li, L. Zhao, Y. Wu, M.S.R. Rajoka, Insights on the ultra high antibacterial activity of positionally substituted 2'-O-hydroxypropyl trimethyl ammonium chloride chitosan: a joint interaction of -NH<sub>2</sub> and -N<sup>(+)</sup>(CH<sub>3</sub>)<sub>3</sub> with bacterial cell wall, *Colloids Surf. B Biointerfaces* 173 (2019) 429–436.
- [23] Q. Chen, Y. Wu, Y. Pu, Z. Zheng, C. Shi, X. Huang, Synthesis and characterization of quaternized beta-chitin, *Carbohydr. Res.* 345 (2010) 1609–1612.
- [24] Y.B. Lee, Y.M. Shin, J.H. Lee, I. Jun, J.K. Kang, J.C. Park, H. Shin, Polydopamine-mediated immobilization of multiple bioactive molecules for the development of functional vascular graft materials, *Biomaterials* 33 (2012) 8343–8352.
- [25] X. Xie, J. Tang, Y. Xing, Z. Wang, T. Ding, J. Zhang, K. Cai, Intervention of polydopamine assembly and adhesion on nanoscale interfaces: state-of-the-art designs and biomedical applications, *Adv. Healthcare Mater.* 10 (2021) e2002138.
- [26] F. Liu, X. Liu, F. Chen, Q. Fu, Mussel-inspired chemistry: a promising strategy for natural polysaccharides in biomedical applications, *Prog. Polym. Sci.* 123 (2021).
- [27] C. Zhang, Y. Ou, W.X. Lei, L.S. Wan, J. Ji, Z.K. Xu, CuSO<sub>4</sub>/H<sub>2</sub>O<sub>2</sub>-Induced rapid deposition of polydopamine coatings with high uniformity and enhanced stability, *Angew Chem. Int. Ed. Engl.* 55 (2016) 3054–3057.
- [28] J. Li, D.J. Mooney, Designing hydrogels for controlled drug delivery, *Nat. Rev. Mater.* 1 (2016).
- [29] N.P. Desai, S.F. Hossainy, J.A. Hubbell, Surface-immobilized polyethylene oxide for bacterial repellence, *Biomaterials* 13 (1992) 417–420.
- [30] L.G. Harris, S. Tosatti, M. Wieland, M. Textor, R.G. Richards, *Staphylococcus aureus* adhesion to titanium oxide surfaces coated with non-functionalized and peptide-functionalized poly(L-lysine)-grafted-poly(ethylene glycol) copolymers, *Biomaterials* 25 (2004) 4135–4148.
- [31] L.K. Ista, H. Fan, O. Baca, G.P. Lopez, Attachment of bacteria to model solid surfaces: oligo(ethylene glycol) surfaces inhibit bacterial attachment, *FEMS Microbiol. Lett.* 142 (1996) 59–63.
- [32] K.W. Kolewe, J. Zhu, N.R. Mako, S.S. Nonnenmann, J.D. Schifman, Bacterial adhesion is affected by the thickness and stiffness of poly(ethylene glycol) hydrogels, *ACS Appl. Mater. Interfaces* 10 (2018) 2275–2281.
- [33] H. Zhu, H. Yang, Y. Ma, T.J. Lu, F. Xu, G.M. Genin, M. Lin, Spatiotemporally controlled photoresponsive hydrogels: design and predictive modeling from processing through application, *Adv. Funct. Mater.* 30 (2020) 2000639.
- [34] B. Bao, Q. Zeng, K. Li, J. Wen, Y. Zhang, Y. Zheng, R. Zhou, C. Shi, T. Chen, C. Xiao, B. Chen, T. Wang, K. Yu, Y. Sun, Q. Lin, Y. He, S. Tu, L. Zhu, Rapid fabrication of physically robust hydrogels, *Nat. Mater.* 21 (2023) 2000252.
- [35] M.A. Watson, J. Lyskawa, C. Zobrist, D. Fournier, M. Jimenez, M. Traisnel, L. Gengembre, P. Woisel, A "clickable" titanium surface platform, *Langmuir* 26 (2010) 15920–15924.
- [36] T.Q. Nguyen, K.L. Tung, Y.L. Lin, C.D. Dong, C.W. Chen, C.H. Wu, Modifying thin-film composite forward osmosis membranes using various SiO<sub>2</sub> nanoparticles for aquaculture wastewater recovery, *Chemosphere* 281 (2021) 130796.
- [37] Y. Yang, X. Liu, Y. Li, Y. Wang, C. Bao, Y. Chen, Q. Lin, L. Zhu, A postoperative anti-adhesion barrier based on photoinduced imine-crosslinking hydrogel with tissue-adhesive ability, *Acta Biomater.* 62 (2017) 199–209.
- [38] X. Yang, J. Yang, L. Wang, B. Ran, Y. Jia, L. Zhang, G. Yang, H. Shao, X. Jiang, Pharmaceutical intermediate-modified gold nanoparticles: against multidrug-resistant bacteria and wound-healing application via an electrospun scaffold, *ACS Nano* 11 (2017) 5737–5745.
- [39] L.K. Hansen, K. Berg, D. Johnson, M. Sanders, M. Citron, Efficacy of local rifampin/minocycline delivery (AIGIS(RX)(R)) to eliminate biofilm formation on implanted pacing devices in a rabbit model, *Int. J. Artif. Organs* 33 (2010) 627–635.
- [40] X. Zhang, G. Zhang, H. Zhang, J. Li, X. Yao, B. Tang, Surface immobilization of heparin and chitosan on titanium to improve hemocompatibility and antibacterial activities, *Colloids Surf. B Biointerfaces* 172 (2018) 338–345.
- [41] P.M. Senna, C.F. de Almeida Barros Mourão, R.C. Mello-Machado, K. Javid, P. Montemezzi, A.A. Del Bel Cury, L. Meirelles, Silane-coating strategy for titanium functionalization does not impair osteogenesis in vivo, *Materials* 14 (2021) 1814.
- [42] H. Chen, L. Zhao, D. Chen, W. Hu, Stabilization of gold nanoparticles on glass surface with polydopamine thin film for reliable LSPR sensing, *J. Colloid Interface Sci.* 460 (2015) 258–263.
- [43] Y. Ma, J. Yao, Q. Liu, T. Han, J. Zhao, X. Ma, Y. Tong, G. Jin, K. Qu, B. Li, F. Xu, Liquid bandage harvests robust adhesive, hemostatic, and antibacterial performances as a first-aid tissue adhesive, *Adv. Funct. Mater.* 30 (2020) 2001820.
- [44] D. Zhao, S. Yu, B. Sun, S. Gao, S. Guo, K. Zhao, Biomedical applications of chitosan and its derivative nanoparticles, *Polymers* (2018) 10.
- [45] J. Carlet, P. Collignon, D. Goldmann, H. Goossens, I.C. Gyssens, S. Harbarth, V. Jarlier, S.B. Levy, B. N'Doye, D. Pittet, R. Richtmann, W.H. Seto, J.W. van der Meer, A. Voss, Society's failure to protect a precious resource: antibiotics, *Lancet* 378 (2011) 369–371.
- [46] H. Cheng, K. Yue, M. Kazemzadeh-Narbat, Y. Liu, A. Khalilpour, B. Li, Y.S. Zhang, N. Annabi, A. Khademhosseini, Mussel-Inspired multifunctional hydrogel coating for prevention of infections and enhanced osteogenesis, *ACS Appl. Mater. Interfaces* 9 (2017) 11428–11439.
- [47] S. Atefyekta, M. Pihl, C. Lindsay, S.C. Heilshorn, M. Andersson, Antibiofilm elastin-like polypeptide coatings: functionality, stability, and selectivity, *Acta Biomater.* 83 (2019) 245–256.
- [48] B.B. Aggarwal, S.C. Gupta, J.H. Kim, Historical perspectives on tumor necrosis factor and its superfamily: 25 years later, a golden journey, *Blood* 119 (2012) 651–665.
- [49] H. Suo, M. Hussain, H. Wang, N. Zhou, J. Tao, H. Jiang, J. Zhu, Injectable and pH-sensitive hyaluronic acid-based hydrogels with on-demand release of antimicrobial peptides for infected wound healing, *Biomacromolecules* 22 (2021) 3049–3059.
- [50] M.D. Turner, B. Nedjai, T. Hurst, D.J. Pennington, Cytokines and chemokines: at the crossroads of cell signalling and inflammatory disease, *Biochim. Biophys. Acta* 1843 (2014) 2563–2582.